Primary Atomization in Water and Kerosene Liquid Sheets At High Pressure

Vital G. Fernandez*, P. Berthoumieu, G. Lavergne
ONERA (French National Aerospace Research Centre)
Heterogeneous Multiphase Flows Unit
Aerodynamic and Energetic Models Department
BO 4025-2, avenue Edouard Belin 31055 Toulouse cedex 4, France

Abstract

In this research, the primary atomization in a liquid sheet was analyzed experimentally. This was generated by a planar airblast atomizer. In order to approach the operating conditions of a turbine engine, the airflow absolute pressure was increased from an atmospheric value to 11 bar. Furthermore, by increasing the air-mass flow rate, the air velocity was kept constant at each pressure condition. Its magnitude went from 20 to 70 m/s. Finally, water and kerosene Jet A1 were injected at an injection velocity of 1 and 2 m/s. The experimental techniques included OLIR (Oscillometry by Laser Intensity Reflexion), LDV (Laser Doppler Velocimetry) and Flow Visualization via a fast camera, with the corresponding image processing, a posteriori. The results presented in this manuscript referred to the global oscillation frequency and the Streamwise ligaments average length. For the former physical quantity an empirical formulation was proposed.

Introduction

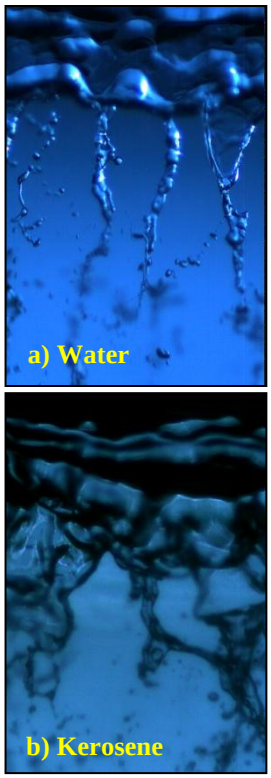

Figure 1. Liquid sheet a) Water b) Kerosene P_{abs} 4 bars, V_{liq} 1m/s, V_{air} 30m/s

In the European Union, the pollutant emissions have increased an 87 % between 1987 and 2006 **[1]**. Furthermore, these same studies, state that the emissions correspond to 2.5% of the total CO_2 production, due to anthropogenic activity. Therefore, it is desirable to improve the combustion in turbine engines, not only for a greater economical feasibility, but as well , for an ecological one.

Nowadays, several approaches are being attempted to reduce CO_2 and NO_X emissions. On one hand, a direct strategy would consist in improving the combustion via a better air-fuel mixing; either mechanically or dynamically. On the other hand, the utilization of bio-fuels could accomplish this purpose indirectly: As the photosynthetic process recuperates the CO_2 from the atmosphere, the overall concentrations in the atmosphere remain constant.

Nevertheless, any of the previous approaches requires a better understanding of the phenomena inside the combustion chamber. Towards this aim, this manuscript presents the research accomplished over the primary atomization. This phenomenon encompasses the physical processes, by which, the continuous injected liquid is disintegrated into isolated structures.

It was one aim of this research, to simulate experimentally, the conditions of a real turbine engine. Towards this end, an airblast atomizer was utilized to generate a planar, 300 μm thin, liquid sheet. Moreover, the airflow pressure was increased from an atmospheric magnitude to 11 bar. Finally, water and kerosene Jet A1 were injected at a velocity of 1 and 2 m/s, **Figure 1**.

Under these parameters, the experimental activity, hereby presented, was characterised by the following non-dimensional ratios: The air Reynolds number went from a transitional value of 1.2×10^5 to a turbulent magnitude of 4.1×10^6 while for the liquids', Reynolds numbers varied between 150 and 600. The We number had a value, which ranged from 1.8 to 23. Eventually, the momentum flux ratio, M, increased from 0.5 to 59. The definition of these numbers can be found in the nomenclature section.

*Vital.Gutierrez_Fernandez@onecert.fr

Materials and Methods

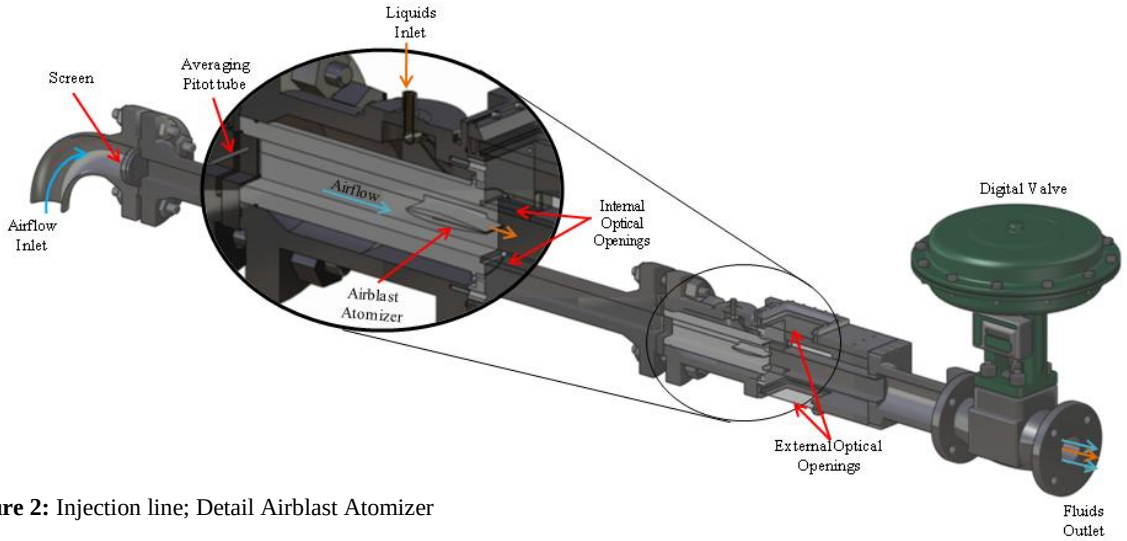

Figure 2: Injection line; Detail Airblast Atomizer

The sketch in **Figure 2** shows the injection line employed in this research. The incoming airflow passed a turbulence screen, followed by a duct, whose length was superior to 30 times its equivalent diameter. This duct had a square cross section of 46x46mm. In the zoomed image, it may be observed how an averaging Pitot-tube was installed, just before the planar airblast atomizer. In order to avoid the effects of recirculation, in the liquid sheet, a second duct was installed after the airblast atomizer. This duct was cut and fit with a couple of optical glasses in order to visualize the liquid flow at the atomizer lips. At the end of the injection line, a pressure valve was used, in combination with manometers and the Pitot-Tube, to control the airflow pressure and velocity at the injection point.

To obtain the data hereby presented, three experimental techniques were applied. The first, named OLIR (Oscillometry by Laser Intensity Reflection), was employed to measure the global oscillation frequency. It consisted in directing a laser beam towards the liquid sheet. Its reflection, at each instant was recorded by a photoreceptor. A FFT of this signal determined the frequency peaks. The second technique consisted in using an LDV (Laser Doppler Velocimetry) system, to determine the boundary layer profile at the injectors' lip. Finally, for each flow configuration, visualizations via a fast camera Phantom v9 were done. The resolution reached for the visualizations was 50 pixels/mm. The initial acquisition rate was 3000 fps. As the liquid sheet became smaller with the airflow pressure increment; it was found convenient to increase the acquisition rate gradually, up to a maximum of 9000 fps, by reducing the images size.

The aim of these visualizations was to study some elements of the liquid sheet, such as the longitudinal ligaments, which could not be characterized by any other technique. Therefore, for measuring these elements, it was required an image processing. In the particular case of the ligaments characterisation, the image processing consisted in two phases: In the first one, the longitudinal ligaments' location was manually selected. The sample population was 128 ligaments, for each flow configuration. The second phase consisted in using a self-written code, which took the form of a plugin for the software ImageJ **[2]**. The diagram in **Figure 3**, shows the operation performed by this program to measure the longitudinal ligaments length and diameter.

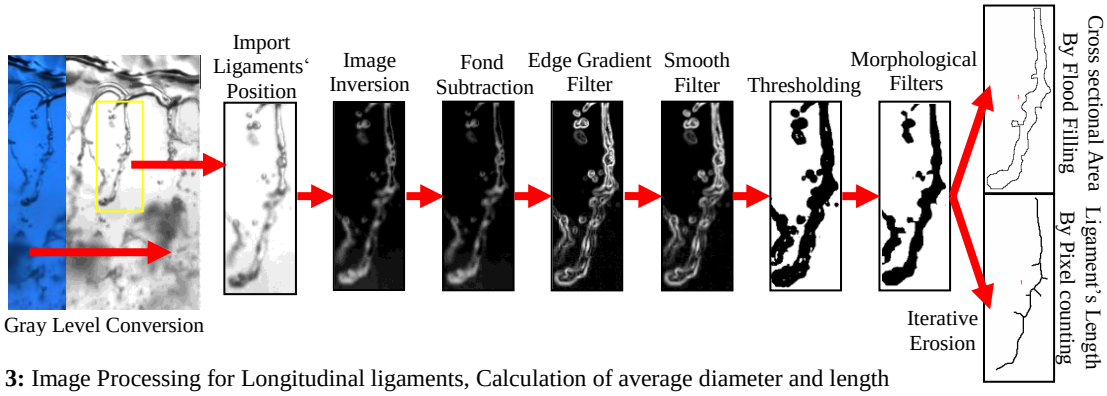

Figure 3: Image Processing for Longitudinal ligaments, Calculation of average diameter and length

Results and Discussion

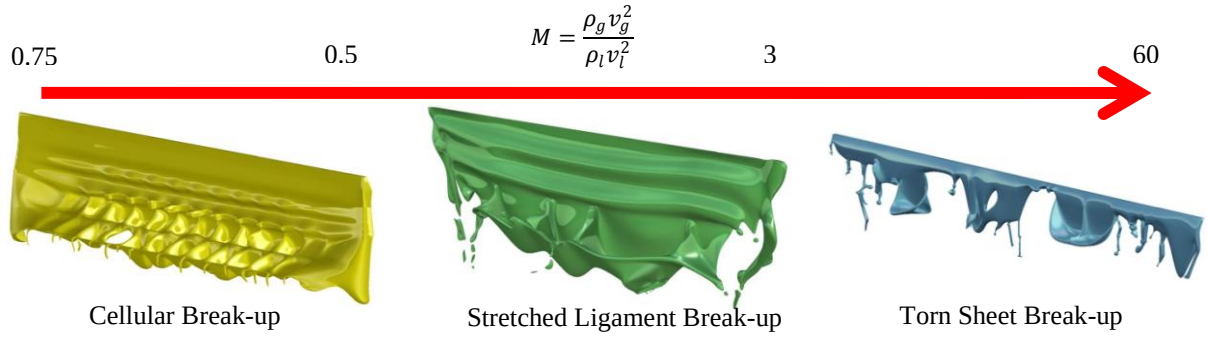

Figure 4: Atomization mechanisms evolution as the momentum flux ratio increased. Boundary values of M for each regime

The diagram in **Figure 4**, shows the atomization mechanisms commonly encountered in the literature. In this research a distinction was made between the diverse *liquid deformations* and the three *atomization mechanisms*, which were observed. The former term includes the different structures developed, when a liquid is submitted to aerodynamic forces. A few examples of these structures included the shaping of a liquid into a flat surface (membrane), into a thin cylinder (ligament), into a low circularity sphere (bulgy droplet)... The latter expression, *atomization mechanisms*, referred to a combination of liquid deformations, originated by a set of fluid instabilities, which disintegrated the continuous liquid flow into isolated droplets. A more throughout discussion of their corresponding peculiarities may be found in **[3].**

It was found that the momentum flux ratio, M, could be used to predict the influence of each atomization mechanism. It should be clarified, that at the flow configurations presented, the mass airflow was increased, correspondently, with the rise in airflow pressure. This was done in order to keep the air velocity constant for each higher pressure.

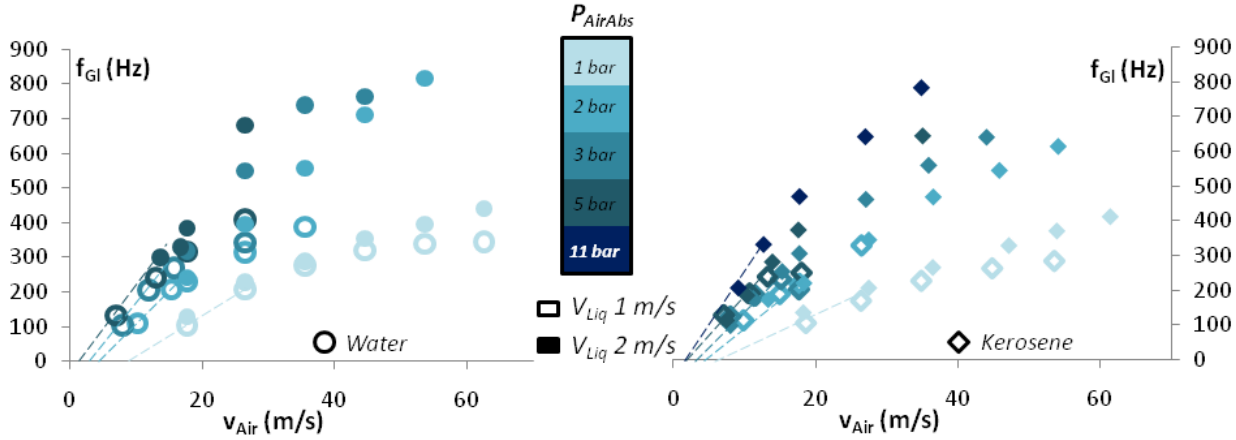

Figure 5. Global Oscillation frequency, a) Water, b) Kerosene

At the lowest values of M: Low airflow velocities at the atmospheric conditions, the cellular break-up **[4]** was predominant. As the fluids' momentum flux ratio got closer to the unity, the stretched ligament break-up influence was the highest. Finally, at high values of the airflow pressure the torn sheet regime was observed. Furthermore, for both liquids, the atomization mechanisms evolution followed the same pattern. The difference lied, however, on the faster evolution for the kerosene; partially due to its lower density. In **Figure 1**, it could be noticed, how for the same flow conditions, there was a greater influence of the torn sheet break-up in the kerosene liquid sheet.

It should be noticed that in an airblast atomizer, there were two fluids in contact, whose densities and velocities are different. Under these conditions, the dynamic behavior of the liquid sheet is dominated by a Kelvin-Helmhotz instability type: As the fluids' interface encouters a perturbation, the airflow comes to a stop, at this local point the static pressure increases; tending to amplify the perturbation. In this system, the surface tension forces acts as the damping element but above a given minimun air velocity, the system became unstable.

This oscillation frequency has been usually termed as global frequency, as it is crutial to determine the generation of droplets at a given flow condition. The graphs in **Figure 5,** show the magnitude of this frequency versus the air velocity, for both liquids' injection velocities and for wide airflow pressure and velocitiy range. The same behaviour was observed in water and kerosene: The frequency was proportional to the air velocity and pressure, while the liquid velocity had a smaller influence in the final frequency value. Nevertheless, for a low liquid injection velocity, the liquid sheet saturated earlier, resulting in a flat frequency histogram. Finally, it may be observed that higher frequency values were found for the kerosene Jet A1 than for water. This was a consequence of its higher dynamic viscosity, which translated into greater shear energy transfer and a lower surface tension, which meant a smaller oscillation damping.

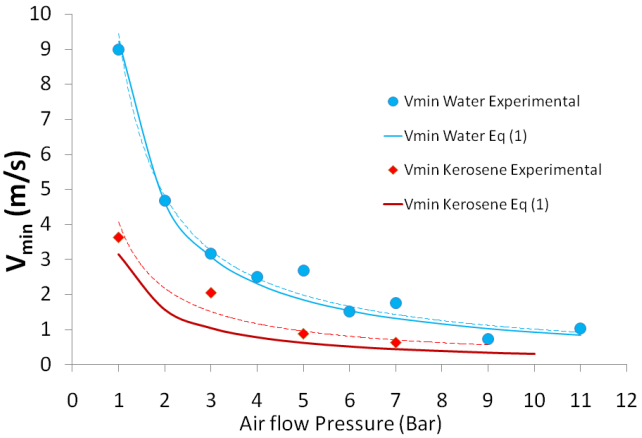

Figure 6 Minimun Air Oscillation Velocity vs Air Pressure

In order to formulate this physical quantity in a non-dimensional format, the Strouhal number has been commonly used. This is due to its suitability to characterise oscillatory flows. While the obvious choice for the characterictic length has been the liquid sheet thickness, a favorised characterictic velocity has remained unchosen. It was Lozano **[5],** who first observed that there was a minimun oscillation velocity for which the liquid sheet started to oscillate. In **Figure 5**, it may be observed, how this velocity was obtained by plotting a trendline for each airflow pressure curve. In this research, it was found that for both fluids this minimun oscillaton velocity could be determine by the following expression:

$$V_{min} = \frac{\sigma_l}{\mu_l}\frac{\rho_l}{\rho_g} 2 \cdot 10^{-4} \qquad (1)$$

In the graph plotted in **Figure 6**, it can be compared the experimental results with those from Eq (1). The previous relation provided a good approximation for both water and kerosene.

In addition, to characterize this physical quantity, knowledge of the airflow boundary layer is necessary. As it has been described before, this oscillation has been commonly explained by a Kelvin-Helmholtz instability type. From a simple to dimensional model **[6]**, it may be learned that this instability growth rate is a function of the relative velocity by vorticity thickness (δ_ω) ratio. This previous parameter was defined as the ratio of the fluids' relative velocity by the airflow velocity gradient at the injectors' lips. Furthermore, in this analysis it is assume that the growth rate is only a function of the streamwise position, for values several times above the longitudinal wavelength. After a dimensional study we found that:

$$St = \frac{f_{Gl}\, t}{v_{min}} = Re_{Air,c_{inj}}\, Oh_t^{\,3/2} \left(\frac{\delta}{\delta_\omega}\right)^{3/2} \qquad (2)$$

Where the Reynolds number accounts for the airflow inertia, the Ohnesorge number includes the fluid physical properties and the boundary layer thickness by vorticity thickness ratio is a measure of the instability growth rate. In **Figure 7**, the Strouhal number was plotted versus the product of the previous dimensionless ratios. The coefficients corresponded to the best fitting. This equation provided a good convergence, at all flow configurations and for both fluids.

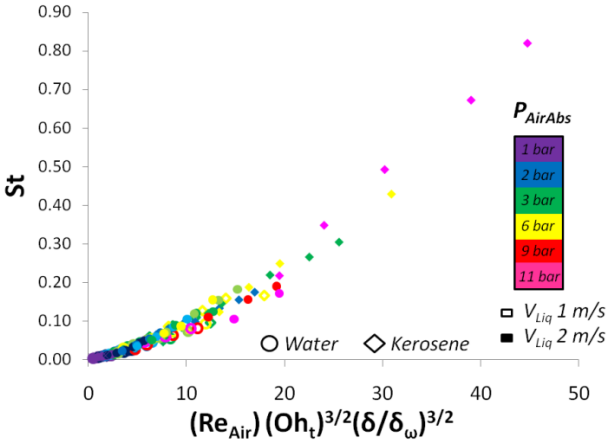

Figure 7 Global Oscillation frequency non-dimensional format Data from all tested conditions

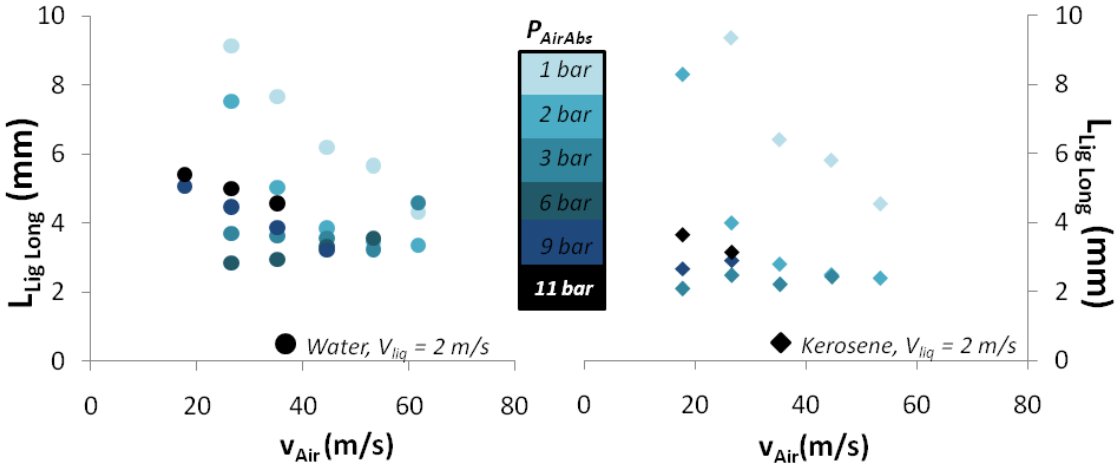

Figure 8. Longitudinal Ligaments average length versus air velocity

As it was showed in **Figure 4**, all the atomization mechanisms observed at the tested conditions developed longitudinal ligaments. These ligaments are a consequence of the airflow, as in similar atomizers, with a still gas phase, these are not generated. Therefore, this liquid deformation characterization is essential not only to determine the droplets generated, but also, to understand the atomization mechanisms behaviour.

The image processing described previously, represented a powerful tool capable to determine both the longitudinal ligaments length and diameter. In the present manuscript only the results of the average longitudinal length will be disused. Nevertheless, it should be said that the average diameter was always below the liquid sheet thickness.

The graphs in **Figure 8**, present the magnitude of the streamwise ligaments length, as a function of the airflow velocity for water (left) and kerosene (right). The values corresponded to a wide pressure range and a liquid injection velocity. For these flow conditions, the atomization mechanisms initially dominant were the Cellular break up and Streched Ligament break-up. The data presented agrees with the visualizations performed: Initially, the longitudinal ligaments length, decreased with the airflow dynamic pressure. Once the momentum flux ratio reached a value around the 5, the ligaments lengths seemed to increase. This was due to a new ligaments population characteristic in the torn sheet regime, with greater lengths and diameters, **Figure 4**. Even with a sample population of 128 ligaments at each flow condition, the data histograms show the expected normal distribution, with a second peak corresponding to these ligaments from the torn sheet break-up. The results showed a similar behaviour for both fluids, the difference lied in the kerosene evolution due to its higher momentum flux ratio, at same flow conditions.

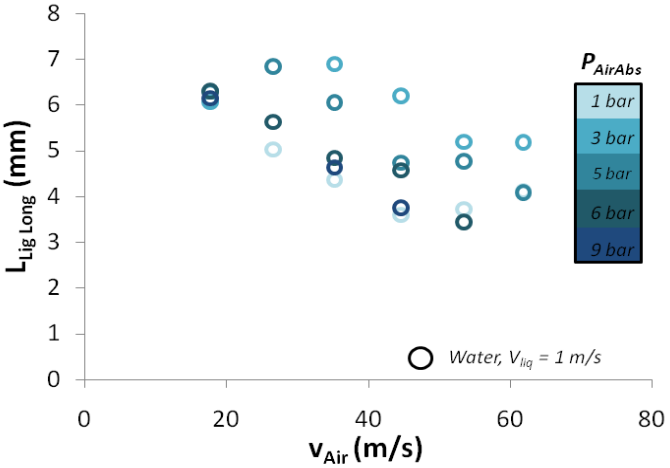

Figure 9. Longitudinal Ligaments length vs Air Velocity

Figure 9, shows similarly presented data for water at an injection velocity of 1 m/s. Unlike in the previous graphs, at these flow conditions, the Torn Sheet break-up had the greatest influence in the liquid sheet behaviour. It may be observed that as the airflow velocity rose, a minimum length was reached (as it did for the case of 2 m/s injection velocity). However, as the pressure increased further, a maximum value was reached. This maximum move to the left as the pressure further increased. This same behaviour was found by, Dumouchel **[8],** for a liquid jet injected in a high pressure chamber with a still airflow**.** It can be concluded that the behaviour of the liquid sheet longitudinal ligaments can be approached by the stability curves of single liquid jets. The position of the ligaments length maximums and minimums depend on the position of the critical liquid velocity and gas density. Similar behaviour was observed for kerosene.

Conclusion

This paper presented an experimental study on two physical quantities, which have a great importance in the primary atomization characterization of an airblast atomizer: the global oscillation frequency and the longitudinal ligaments length. These measurements were accomplished for a wide value of air and liquid velocities, airflow pressures for both water and kerosene Jet A1. It was concluded from the data obtained that:

a) The global oscillation frequency had its magnitude increased with the raise in airflow pressure. Still, it showed the same behaviour at every atomization mechanisms. The minimum air velocity, at which this oscillation started, was found to be predicted by the fluids physical properties.

b) The values for the longitudinal ligaments length in the stretched ligament break-up and cellular break-up showed the same behaviour: they decreased in magnitude, as the dynamic pressure increased. However, it was observed in the flow visualizations, as well as in the quantitative measurements that, from a certain value of the momentum flux ratio (around 3), the average length would start to increase. Furthermore, similar behaviour for was observed between the liquid jets of Dumouchel, at high pressure, and the longitudinal ligaments in a liquid sheet. Future research will consist in a PIV study to determine the liquid flow velocity, and hence, obtain the stability curves for these ligaments, to confirm this theory.

Nomenclature

c_{inj}	Airblast Chord Length				
D	Diameter				
t	Liquid sheet thickness				
f_{Gl}	Global Oscillation Frequency				
l	length				
v_g	Gas Velocity				
v_l	Liquid Velocity				
V_{min}	Minimum Air Oscillation velocity				
δ	Boundary layer thickness				
δ_ω	Vorticity thickness				
μ_g	Gas Dynamic Viscosity	Air	1.825×10^{-5} kg/ms		(15ºC)
μ_l	Liquid Dynamic Viscosity	Kerosene	2.317×10^{-3} kg/ms	Water 1.03×10^{-3} kg/ms	(15ºC)
ρ_g	Gas density	Air	1.224 kg/m^3		(15ºC)
ρ_l	Liquid density	Kerosene	818.8 kg/m^3	Water 998 kg/m^3	(15ºC)
σ	Surface Tension	Kerosene	2.52×10^{-2} kg/s^2	Water 7.28×10^{-2}kg/s^2 (15ºC)	

Subscripts

air	airflow
g	gas
l	liquid
lig	ligament

Non-dimensional Ratios

$M = \rho_g v_g^{\,2}/\rho_g v_g^{\,2}$	Momentum flux ratio
$Re_{Air} = \rho_g v_g c_{inj}/\mu_g$	Air Reynolds number
$Re_{Water} = \rho_l v_l\, e_{l\,j}/\mu_l$	Water Reynolds number
$We = \rho_g\, v_g^{\,2} c_{inj}/\,\sigma$	Weber Number
$St = f_{Gl}\, t/v_{min}$	Strouhal Number

References

1. EU Press release (2006-12-20) *Climage Change: Commission proposes bringing air transport into Emissions' Trading Scheme*, Retrieved on 2008-01-02
2. Rasband, W.S., *ImageJ, U.S. National Institutes of Health*, Bethesda, Maryland, USA, http://rsb.info.nih.gov/ij/
3. V G Fernández, P. Berthoumieu, G. Lavergne, "Liquid Sheet Disintegration At High Pressure : Experimental Approach", Colloque INCA (Advance Combustion INntiative), 2008
4. Stapper B.E, Sowa W. A. And Samuelsen G. S., "An Experimental Study of the Effects of Liquid Properties on the Break-up of a two-dimensional Liquid Sheet", Gas turbine and Aeroengine Congress and Exposition, 1990.
5. Lozano A., Félix Barreras, Guillermo Hauke and César Dopazo, "Longitudinal Instabilities in a liquid sheet", J.Fluid Mech (2001), vol 437, pp 143-173, 2000
6. F. Charru, Instabilité non visqueuse des écoulements parallèles, in Intabilités Hydrodynamiques, EDP Sciences/CNRS Editions, France, 2007
7. Villermaux E., Marmottant, "Fragmentation of stretched liquid ligaments". Université de Provence, Physics of Fluids vol. 16 num 8, August 2004
8. S. Leroux, C. Dumouchel, and M. Ledoux, The Stability Curve of Newtonian Liquid jets, Atomization and Sprays, Vol. 6, no. 6, pp 623-647, 1996 .